

WHIS: Hearing impairment simulator based on the gammachirp auditory filterbankToshio Irino^{1, a)}*Faculty of Systems Engineering, Wakayama University, 930 Sakaedani Wakayama,
640-8510, Japan*

A new version of a hearing impairment simulator (WHIS) was implemented based on a revised version of the gammachirp filterbank (GCFB), which incorporates fast frame-based processing, absolute threshold (AT), an audiogram of a hearing-impaired (HI) listener, and a parameter to control the cochlear input-output (IO) function. The parameter referred to as the compression health α controlled the slope of the IO function to range from normal hearing (NH) listeners to HI listeners, without largely changing the total hearing loss (HL). The new WHIS was designed provide an NH listener the same EPs as those of a target HI listener. The analysis part of WHIS was almost the same as that of the revised GCFB, except that the IO function was used instead of the gain function. We proposed two synthesis methods: a direct time-varying filter for perceptually small distortion and a filterbank analysis-synthesis for further HI simulations including temporal smearing. We evaluated the WHIS family and a Cambridge version of the HL simulator (CamHLS) in terms of differences in the IO function and spectral distance. The IO functions were simulated fairly well at α less than 0.5 but not at α equal to 1. Thus, it is difficult to simulate the HL when the IO function is sufficiently healthy. This is a fundamental limit of any existing HL simulator as well as WHIS. The new WHIS yielded a smaller spectral distortion than CamHLS and was fairly compatible with the previous version.

Keywords: Hearing loss, Hearing impairment, Auditory filterbank, Cochlear model,

Peripheral dysfunction

^{a)} irino@wakayama-u.ac.jp

I. INTRODUCTION

As many countries approach the super-aging society status, the number of hearing-impaired (HI) listeners may increase. It is crucial to develop next-generation assistive devices that can compensate for the difficulties faced by individual HI listeners. For this purpose, it is essential to effectively specify the dysfunctions without a heavy experimental load. Many psychoacoustic experiments have been conducted to clarify the dysfunctions using relatively simple stimulus sounds, such as sinusoids and noise (Moore, 2013). In addition, many speech sound experiments have been performed, although they have mainly been restricted to intelligibility tests, such as speech-in-noise tests. However, in experiments conducted with elderly HI listeners, it is not easy to specify whether the deterioration factor is located on the periphery, the auditory pathway, or cognition. This is because of the huge variability among HI listeners in terms of both audiograms and cognitive factors.

To resolve this problem, at least partially, a hearing loss (HL) simulator was developed to specify the effects of the peripheral dysfunction, such as elevation of absolute threshold (AT) and loudness recruitment, on speech intelligibility (Villchur, 1974). Normal-hearing (NH) listeners could evaluate the speech intelligibility of the HL-simulated sounds, which might correspond to what HI listeners perceive. In the HL simulator, input signals were decomposed into frequency bands by using a set of linear filters, and then expanded and synthesized to obtain the simulated signal. Moore and Glasberg (1993) initially introduced auditory filters into an HL simulator for loudness recruitment and a more precise simulation of the frequency selectivity. The auditory filters were psychoacoustically estimated by conducting notched-noise (NN) masking experiments (Patterson, 1976) for both NH and HI listeners (Glasberg and Moore, 1986; Patterson *et al.*, 1982). An rounded exponential (roex) filter was used in the estimation. Spectrum smearing was introduced to evaluate the effect of the bandwidth widening in an HI listener’s auditory filter (Baer and Moore, 1993, 1994). In addition, a unified version was developed to include loudness recruitment and spectrum smearing (Nejime and Moore, 1997). This Cambridge version of the HL simulator is referred to as CamHLS. CamHLS was used in a study of the upper limit of temporal delay in hearing aids (Stone and Moore, 1999). Recently, CamHLS has also been used in the base line system of “Clarity Prediction Challenge” (CPC1) (Clarity Challenge, 2021), which is a competition conducted to develop a new objective measure for hearing-aid signal processing. There are other HL simulators as well. For example, HeLPS v2 (Zurek and Desloge, 2007) is commercially available and includes the simulation of loudness recruitment. We also developed another type of HL simulator (Irino *et al.*, 2013; Irino and Patterson, 2020; Nagae *et al.*, 2014), which is referred to as the Wakayama-University Hearing Impairment Simulator (WHIS), which is based on a dynamic compressive gammachirp filterbank (GCFB) (Irino

and Patterson, 2006). The gammachirp filter in GCFB is a time-domain filter, unlike the roex filter, which accounts for the NN masking thresholds fairly well (Irino and Patterson, 1997; Patterson *et al.*, 2003). The gammachirp requires smaller number of coefficients than the roex filter (Unoki *et al.*, 2006). Based on this psychoacoustical backgrounds, GCFB was also used in an HL simulator functionally similar to CamHLS (Hu *et al.*, 2011) and a real-time HL simulator (Grimault *et al.*, 2018). WHIS was designed to control the degree of the compression in the cochlear input-output (IO) function rather than to simulate the loudness recruitment directly. WHIS has been used in various experimental studies as described in the Discussion section.

However, HL simulators have been mostly used in speech intelligibility studies. This is probably because the simulated sounds contain more or less distortion components, which preclude precise psychoacoustic experiments and sound quality evaluations. Although the distortion is unavoidable due to nonlinear signal processing in nature, it can be reduced to a sufficiently small level with sophisticated processing. For this purpose, a goodness measure of the HL simulator is required. It is also important to know the fundamental limit of the HL simulator. To the best of our knowledge, there have been no reports on such measures and comparisons between HL simulators. Although these HL simulators were developed to simulate the peripheral dysfunction, more central temporal resolution or temporal modulation transfer function (TMTF) (Bacon and Viemeister, 1985) is an important factor for speech perception (Drullman *et al.*, 1994). Thus, it is desirable to simulate both the peripheral and central dysfunctions within a unified framework.

In this study, a new version of WHIS, based on an improved version of GCFB, is developed to address these issues. The new GCFB is first explained as it improved in processing speed and incorporated the audiogram and compression characteristics of HI listeners. Then, the analysis and synthesis methods of WHIS are described based on the signal processing of GCFB. WHIS and CamHLS are evaluated using spectral distance and IO function. Finally, we discussed the fundamental limit of HL simulators, estimation of the active and passive HLs, and applications of WHIS.

II. IMPROVEMENT IN GCFB

WHIS was developed based on a compressive gammachirp filter (cGC) (Irino and Patterson, 2001) and a dynamic compressive gammachirp filterbank (GCFB) (Irino and Patterson, 2006). For the implementation of the new WHIS, GCFB should be improved to meet the following WHIS specifications, 1) fast frame-based processing for an interactive user inter-

face, 2) clear definition of the cochlear output level relative to the AT, and 3) incorporation of the audiograms and cochlear IO functions of HI listeners.

In this section, we first define a cGC filter then explain its improvement in detail. Although it is somewhat lengthy, it is essential to understand the concept of the new GCFB-based WHIS.

A. cGC filter

The background of a cGC developed from the original gammachirp was reviewed by [Irino and Patterson \(2020\)](#). The absolute frequency response of a cGC ([Irino and Patterson, 2001](#)), $|G_{CC}(f)|$, can be formulated as

$$|G_{CC}(f)| = |G_{CP}(f)| \cdot H_{HPAF}(f). \quad (1)$$

Here

$$|G_{CP}(f)| = a_{\Gamma} |G_T(f)| \exp(c_1 \theta_1), \quad (2)$$

$$H_{HPAF}(f) = \exp(c_2 \theta_2), \quad (3)$$

$$\theta_1 = \arctan\left(\frac{f - f_{r_1}}{b_1 \text{ERB}_N(f_{r_1})}\right), \quad (4)$$

$$\theta_2 = \arctan\left(\frac{f - f_{r_2}}{b_2 \text{ERB}_N(f_{r_2})}\right). \quad (5)$$

$|G_{CC}(f)|$ is a product of a passive gammachirp (pGC), $|G_{CP}(f)|$, and a high-pass asymmetric filter (HP-AF), $H_{HPAF}(f)$, which enables the level-dependent control of bandwidth and gain and is formulated as $\exp(c_1 \theta_1)$. $|G_{CP}(f)|$ is a product of a gammatone $|G_T(f)|$ and $\exp(c_1 \theta_1)$ which introduces a frequency glide or chirp. The scalar value a_{Γ} is the amplitude; b_1 and b_2 are bandwidth factors; c_1 and c_2 are chirp factors; and f_{r_1} and f_{r_2} are the asymptotic frequency of pGC and the center frequency of HP-AF, respectively. $\text{ERB}_N(f)$ is an equivalent rectangular bandwidth of NH listeners at frequency f ([Moore, 2013](#)).

When the peak frequency of a pGC is f_{p1} and the sound pressure level at the pGC output is estimated as P_{gcp} on a dB scale, the center frequency of HP-AF, the center frequency of HP-AF, f_{r_2} , is associated with f_{p1} to introduce the level dependency of a cGC.

$$f_{r_2} = f_{rat}(P_{gcp}) \cdot f_{p1}, \quad (6)$$

$$f_{rat}(P_{gcp}) = f_{rat}^{(0)} + f_{rat}^{(1)} \cdot P_{gcp}, \quad (7)$$

where $f_{rat}^{(0)}$ and $f_{rat}^{(1)}$ are coefficients which are estimated together with the other parameters, b_1, c_1, b_2 , and c_2 , by conducting the NN masking experiments ([Irino and Patterson, 2001](#)).

The parameter values reported by (Patterson *et al.*, 2003) are used in this study: $b_1 = 1.81$; $c_1 = 2.96$; $b_2 = 2.17$; $c_2 = 2.20$; $f_{rat}^{(0)} = 0.466$; $f_{rat}^{(1)} = 0.0109$.

B. Introduction of frame-based processing into GCFB

The original version of GCFB (hereafter, GCFB_{v21}) was developed using the cGC formula to simulate cochlear filtering (Irino and Patterson, 2006). The level-dependent filtering in GCFB_{v21} required heavy computational costs because the filter coefficients in many channels were updated and convoluted with the input signal at each sample point. The duration required for this sample-by-sample processing was several tens to a hundred times of the input signal duration. Therefore, it could not be used as a background processor for the interactive human interface necessary in WHIS. This problem did not occur in the previous version of WHIS (hereafter WHIS_{v22}), as it used several approximations. In the new version of WHIS (hereafter WHIS_{v30}), hearing loss (HL) was simulated on the basis of excitation patterns (EPs) from input signals, as described in the next section. The EPs can be calculated as short-time averaged levels of filterbank outputs and does not require sample-by-sample processing. Therefore, frame-based processing was introduced into the new version of GCFB (hereafter GCFB_{v23}). As the filtering was performed in every frame of a few millisecond, it was possible to improve the processing speed. Although the temporal fine structure (TFS) was discarded in the frame-based processing, it could be calculated in the sample-by-sample circuit inherited from GCFB_{v21} if necessary.

C. Block diagram of GCFB

Figure 1 shows a block diagram for one GCFB_{v23} channel. We provide an overview of the signal flow here before describing the individual components in the following sections. As in GCFB_{v21}, there are two paths for level estimation (upper block) and signal flow (bottom block), both of which have the same linear pGC and HP-AF filters, except for the center frequencies. Outputs of the level estimation path were used to estimate the signal level, P_c , by using hanning windows, where the rms level was calculated with a window length of 1 ms and frame-shift of 0.5 ms. The method for the level estimation using two signal sources (i.e., s_1 and s_2) was almost the same as that used for GCFB_{v21}. The frame-based level, P_c , determined the gain value of an active gain function (right-middle block). The output of the linear filters in the signal path (bottom block) can also be summarized using the same hanning window. The frame-based signal level was, then, controlled by the active

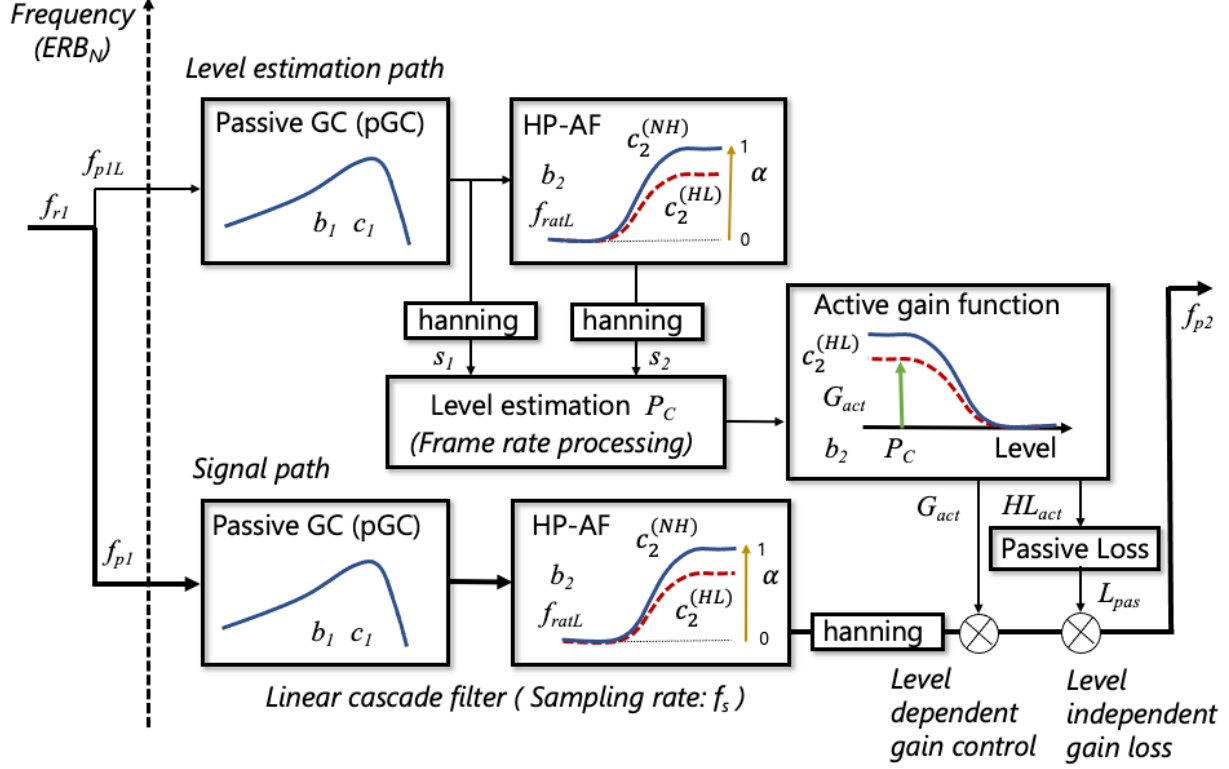


FIG. 1. Block diagram of one channel of the frame-based GCFB, GCFB_{v23}

gain function to produce the output. The elapsed time for this frame-based processing was roughly the same as the input signal duration when using MATLAB. The short processing time is essential for WHIS and can be useful for various applications that do not require TFS.

D. Introduction of the HL into GCFB

We explain the basic concept of how to introduce the HL into the model.

1. Audiogram and HL

The peripheral HL of an HI listener can be modelled using the dysfunctions in the active and passive processes. We assumed the total HL, HL_{total} , as the sum of the active HL, HL_{act} , and the passive HL, HL_{pas} , on a dB scale:

$$HL_{total} = HL_{act} + HL_{pas}. \quad (8)$$

Moore *et al.* (1997) proposed a similar equation on a dB scale, $HL_{total} = HL_{OHC} + HL_{IHC}$, where HL_{OHC} is the HL caused by the outer hair cell (OHC) and HL_{IHC} is that caused by the inner hair cell (IHC). Although the main concept for both equations is almost the same, Eq. 8 is preferred in this paper because the active process is not solely functioned by the OHC and the passive loss is not solely caused by the IHC dysfunction.

2. Introduction of compression health

cGC in Eq.1 comprises pGC, which represents a passive filter, and HP-AF, which represents an active mechanism. We assumed that pGC is common to both NH and HI listeners because it is a broadband filter that could simulate the response of cochlear traveling wave at high sound pressure levels (SPLs). The dysfunction of the active process could be modelled by reducing the dynamic range of HP-AF in Eq.3, which is determined by the coefficient c_2 . The original value of c_2 is estimated from the NN thresholds of NH listeners ($c_2^{(NH)}$). The c_2 values for HI listeners might be smaller because of the active HL ($c_2^{(HL)}$). We introduced a coefficient α $\{0 \leq \alpha \leq 1\}$ and defined the relationship between $c_2^{(NH)}$ and $c_2^{(HL)}$ as

$$c_2^{(HL)} = \alpha \cdot c_2^{(NH)}. \quad (9)$$

At $\alpha = 1$, there is no dysfunction in the active process and this is the case for NH listeners. At $\alpha = 0$, the active function is completely damaged. The value for an individual HI listener can be somewhat in the middle and frequency-dependent. We can control the α value based on the measurement or assumption about the degree of compression in the cochlear IO function, as described in the Discussion section. Thus, the parameter α is referred to as “compression health.” Although the definition and value are different from those of the compression health α defined in WHIS_{v22} (Irino and Patterson, 2020), both α s are highly correlated.

The HP-AF of an HI listener could be represented as

$$H_{HPAF}^{(HL)}(f) = \exp(c_2^{(HL)}\theta_2) = \exp(\alpha \cdot c_2^{(NH)}\theta_2). \quad (10)$$

Two HP-AF curves when using $c_2^{(NH)}$ and $c_2^{(HL)}$ are depicted in the HP-AF blocks of Fig.1. The dynamic range of HP-AF reduces as α reduces. The amplitude spectrum of cGC for an HI listener is represented as

$$|G_{CC}^{(HL)}(f)| = |G_{CP}(f)| \cdot H_{HPAF}^{(HL)}(f). \quad (11)$$

As indicated in the previous section, pGC and HP-AF are implemented as linear filters for speed-up. The frequency relationship between pGC and HP-AF is set by Eq.7 with P_{gcp}

fixed at approximately 50 dB. The peak gain is normalized to 0 dB independently of the parameter $c_2^{(HL)}$. The impulse response is formulated as

$$g_{cc}^{(HL)}(t) = g_{cp}(t) * h_{HPAF}^{(HL)}(t), \quad (12)$$

where $h_{HPAF}^{(HL)}(t)$ is an approximation filter of $H_{HPAF}^{(HL)}(f)$ which does not have phase information (Irino and Patterson, 2006). This linear cascade filter does not represent level-dependent gain and bandwidth in accordance with the input sound level. However, the bandwidth difference between NH and HI listeners can be modeled by using α . The level-dependent gain is introduced by the active gain function (right-middle block), as shown in Fig. 1. The gain value $G^{(HL)}$ is determined from the estimated signal level $P_c(\tau)$, which is derived at each frame time τ . Eq. 12 can be rewritten by using $G^{(HL)}(P_c(\tau))$ as

$$g_{cc}^{(HL)}(\tau) = W_{han}\{g_{cp}(t) * h_{HPAF}^{(HL)}(t)\} \cdot G^{(HL)}(P_c(\tau)), \quad (13)$$

where $W_{han}\{\cdot\}$ denotes the rms calculation performed using the hanning window, which resamples the signal sampling rate to the frame rate, as shown in Fig. 1.

The gain $G^{(HL)}(P_c(\tau))$ is calculated by using Eqs. 3 and 5, as follows:

$$G^{(HL)}(P_c(\tau)) = H_{HPAF}^{(HL)}(f_{p1}, P_c(\tau)) \quad (14)$$

$$= \exp\left\{c_2^{(HL)} \cdot \arctan\left(\frac{f_{p1} - f_{r2}}{b_2 \text{ERB}_N(f_{r2})}\right)\right\}$$

$$f_{r2} = f_{rat}(P_c(\tau)) \cdot f_{p1} \quad (15)$$

where f_{p1} is the peak frequency, f_{r2} is the center frequency of HP-AF, and $f_{rat}(P_c(\tau))$ is similar to Eq. 6 but with the frame-based estimated level $P_c(\tau)$.

The gain of the active process decreases as the input SPL increases, as observed in the cochlear IO function. When a high SPL that yields the active gain of 0 dB is denoted as P_{gain0} (e.g., 100 dB), the active gain G_{act} can be approximated as

$$G_{act}(P_c(\tau)) = \frac{H_{HPAF}(f_{p1}, P_c(\tau))}{H_{HPAF}(f_{p1}, P_{gain0})}. \quad (16)$$

This equation is valid for both NH and HI listeners because P_{gain0} is assumed to be the same for both. The only difference is whether $c_2^{(NH)}$ or $c_2^{(HL)}$ should be used for calculating $H_{HPAF}(f_{p1}, P_c(\tau))$.

3. Cochlear IO function and HL

Figure 2 shows a schematic graph of the cochlear IO functions to explain the effects of the active and passive dysfunctions. The horizontal axis is the input level (SPL dB) to the

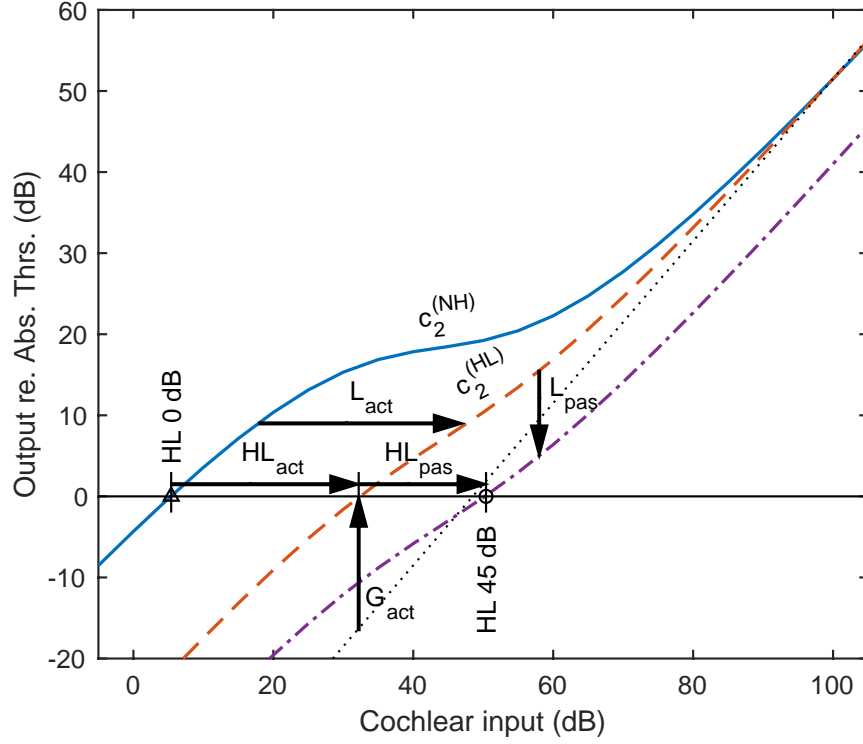


FIG. 2. Schematic plot of the cochlear IO function. The abscissa is the SPL (dB) at the cochlear input. The ordinate is the output level (dB) relative to the AT. The label “HL 0 dB” represents the input level corresponding to the AT of the average NH listener as defined in (ANSI/ASA S3.6 - 2018, 2018). The blue solid line represents the IO function of the NH listener. The black dotted line shows a linear relationship or 1:1. The orange dashed line shows the IO function when using $c_2^{(HL)}$ and $\alpha = 0.5$ without any passive HL. Then, the threshold increases for HL_{act} from HL 0 dB. When the passive HL exists, the line moves downward for L_{pas} . The purple dashed-and-dotted line shows the IO function of an HI listener whose hearing level is 45 dB as an example. The AT further decreases for HL_{pas} . Thus $HL_{act} + HL_{pas} = 45$ dB in this case. L_{act} is used in WHIS and is described by Eq. 24.

cochlea, and the vertical axis is the output level (dB) relative to that for the AT or “HL 0 dB,” which is calculated from the hearing level defined in [ANSI/ASA S3.6 - 2018 \(2018\)](#) and a transfer function between the middle ear and the cochlear input, which is used in a loudness model proposed by [Glasberg and Moore \(2006\)](#). “HL 0 dB” is located at the intersection of the IO function of the average NH listener (blue solid line labeled with $c_2^{(NH)}$) and the horizontal 0-dB line. This IO function has linear growth in the low SPLs becomes compressive in the middle SPLs, and then converges onto a 1:1 linear function (dotted line) in the high SPLs. The hearing level of an HI listener is located on the right of “HL 0 dB” on the horizontal 0-dB line.

First, let us consider a case in which the HL is solely caused by the active dysfunction. When we use $c_2^{(HL)}$ with α value of 0.5 instead of $c_2^{(NH)}$, in Eqs. 10 and 16, the IO function becomes the red dashed line, which is steeper and less compressive. The difference between the IO functions of $c_2^{(NH)}$ and $c_2^{(HL)}$ result in the elevation of the AT for HL_{act} from “HL 0 dB” on the horizontal 0-dB line. Then, by introducing the passive dysfunction, the IO function moves downward for L_{pas} to the purple dashed-and-dotted line, which represents the case of, for example, an HI listener whose hearing level is 45 dB (“HL 45 dB”). Then, the AT elevated for HL_{pas} . It is a rationale of Eq. 8 in which HL_{total} (45 dB in this case) is a sum of HL_{act} and HL_{pas} .

Using this framework, the ratio between HL_{act} and HL_{pas} can be controlled without changing HL_{total} . We can specify the HL of an HI listener, HL_{total} , from the audiogram and α in advance. The active gain G_{act} and HL_{act} are automatically determined from the IO function as described above. Then, HL_{pas} is determined as $HL_{pas} = HL_{total} - HL_{act}$ from Eq. 8.

4. Implementation in GCFB

In GCFB_{v23}, the active gain, G_{act} , and the passive loss, L_{pas} (> 0), are calculated in the active gain function block and the successive block shown on the right side of Fig. 1. The total gain applied to the output of the linear pGC and HP-AF filters is

$$G_{total}(P_c(\tau)) = G_{act}(P_c(\tau)) - L_{pas} \quad (17)$$

on a dB scale. Note that $G_{act}(P_c)$ is level-dependent while L_{pas} is a constant that is determined from HL_{pas} and the IO function. This process is performed in every filterbank channel n_{ch} with the estimated signal level $P_c(n_{ch}, \tau)$. Equation 17 is rewritten more specifically as

$$G_{total}(n_{ch}, P_c(n_{ch}, \tau)) = G_{act}(n_{ch}, P_c(n_{ch}, \tau)) - L_{pas}(n_{ch}). \quad (18)$$

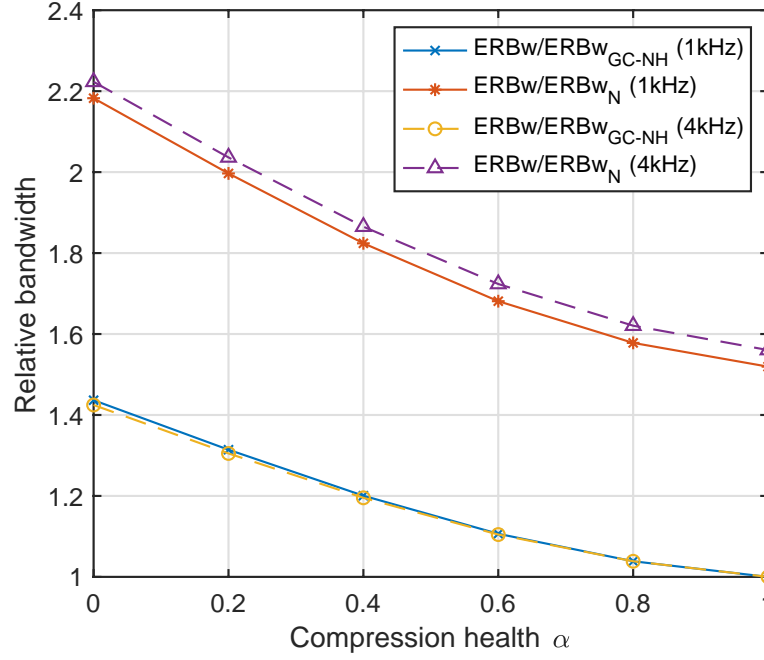


FIG. 3. Filter bandwidth as a function of the compression health, α . Solid lines: 1 kHz. Dashed lines: 4 kHz. The two lower lines show the bandwidth relative to the case when $\alpha = 1$ in GCFB_{v23}. The two upper lines show the bandwidth relative to the standard ERB_N bandwidth of the average NH listener (Moore, 2013).

E. Simulation results

The simulations using GCFB_{v23} are performed to evaluate the algorithms described above.

1. Evaluation of bandwidth

As described previously, the pGC and HP-AF filters are implemented as linear filters for speed-up. The filter shapes of HI and NH listeners are determined from the value of α . Although the level dependence is not implemented in this formulation, it might not be entirely unreasonable, at least when simulating the HI listener's filter, because the nonlinearity is smaller in HI listeners than in NH listeners.

Figure 3 shows the bandwidth of the cascade filter (pGC + HP-AF) as a function of α at signal frequencies of 1 kHz and 4 kHz. The vertical axis is the relative bandwidth normalized by the bandwidth at $\alpha = 1$ (i.e., a completely healthy condition). The lower curves show that, as α decreases from 1.0 to 0, the bandwidth increases gradually from 1.0 to 1.4 times. At $\alpha = 0$, it is the bandwidth of the pGC filter because the frequency response of the HP-AF filter is unity (0 dB), as indicated in Eq.10.

When the bandwidth is normalized by the standard ERB_N bandwidth (Moore, 2013), the relative bandwidth is 1.6 times wider than the value calculated above. This is because the bandwidth of the cGC filter estimated with the NN masking paradigm by Patterson *et al.* (2003) is wider than $ERB_N(f)$ at any SPL, and the current cascade filter is fixed at the characteristics of approximately 50 dB SPL. The bandwidth difference between NH and HI listeners is introduced in $GCFB_{v23}$ although the degree of the difference is arguable. The values can be compensated by changing the coefficients of cGC and GCFB, based on a more precise estimation of the auditory filter.

2. Evaluation of IO function

The IO function of $GCFB_{v23}$ might not correspond to the schematic function shown in Fig.2, because of the introduction of several approximations, such as frame-based processing and the impulse response in Eq.12. Therefore, we calculate the IO functions of $GCFB_{v23}$ under the NH condition and three HI conditions at the audiogram frequencies between 125 and 8000 Hz. The HL of the HI listener is set to the average value of 80 year-old males (Tsuiki *et al.*, 2002). The value of α is set to 0.0, 0.5, and 1.0 to show the difference, because the audiogram does not provide information about it. The practical values of α are different from 0, even when setting $\alpha = 0$ in advance, because the minimum value of α is restricted by HL_{total} . The values are listed in Table I in the parentheses (compensated α).

Figure 4 shows the IO functions between 250 and 8000 Hz. The input signals are sinusoids of 200 ms duration with the level of every 10 dB step from -10 to 100 dB. The outputs are the maximum values of the EPs calculated by GCFB.

The IO functions of the NH listener (blue solid line) intersect the horizontal 0-dB line near the points labeled with “HL 0 dB” (triangles). The differences between the zero cross points and “HL 0 dB” are listed in the second row of Table I. The maximum difference is 4.6 dB at 2000 Hz, and thus, smaller than 5 dB, which is the resolution of a normal audiometry test.

The IO functions of the HI listener at $\alpha = 1$ (green dashed line) are shifted down for L_{pas} without changing the shapes of those of the NH listener. Therefore, they have compressive regions. The differences between the zero cross points and the HL values of the HI listener

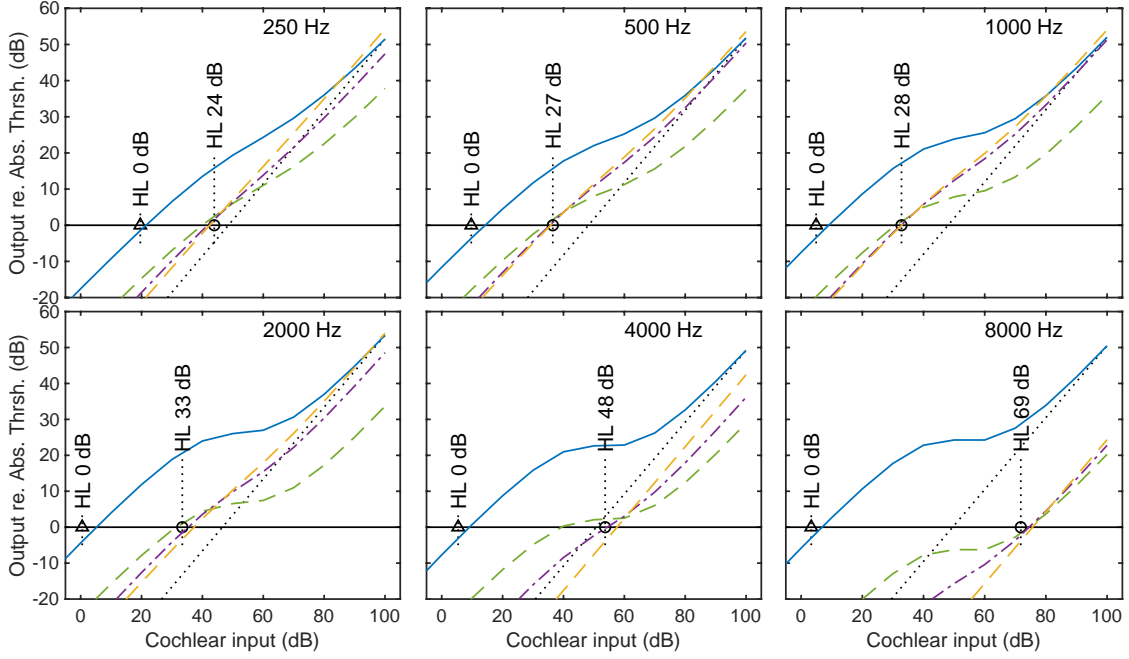


FIG. 4. Simulation results on the IO function for frequencies between 250 and 8000 Hz. The abscissa is the SPL (dB) at the cochlear input. The ordinate is the output level (dB) relative to the AT. HL 0 dB corresponds to the AT of average NH listeners ([ANSI/ASA S3.6 - 2018, 2018](#)). The other HL values are derived from the average HL of 80-year-old male listeners reported by [Tsuiki *et al.* \(2002\)](#). Blue solid line: Average NH. Green dashed line: HL with the compression health α of 1.0. Purple dashed-and-dotted line: HL with α of 0.5. Orange dashed line: HL with α of 0.0. Black dotted line: The linear relationship (1:1).

are listed in the third row of Table I. The absolute differences are less than 5 dB, except at 4000 Hz, where the compressive region is very close to the horizontal 0-dB line, which increases the difference. The IO functions are much steeper at $\alpha = 0.5$ (purple dashed and dotted lines) and $\alpha = 0.0$ (orange dashed lines) than at $\alpha = 1.0$. The steep function can cause the loudness recruitment. The differences between the zero cross points and the HL values are listed in the fourth and fifth rows. Most of them are less than 5 dB. The maximum absolute difference at 125 Hz is less than 10 dB. The results demonstrated that the output level at the AT is set to 0 dB in GCFB_{v23} fairly well for both NH and HI

TABLE I. Difference (dB) between the zero cross point of the IO function and the average hearing levels of NH and HI listeners in Fig.4. The hearing level of average 80-year-old HI listeners (Tsuiki *et al.*, 2002) is shown in the bottom row. The simulations were performed for α values of 0.0, 0.5, and 1.0.

| Freq. (Hz) | 125 | 250 | 500 | 1000 | 2000 | 4000 | 8000 |
|-------------------------|-------|--------|--------|--------|--------|-------|-------|
| NH ($\alpha = 1$) | -2.1 | 1.3 | 4.2 | 3.9 | 4.6 | 3.6 | 3.5 |
| HI ($\alpha = 1$) | -4.5 | -4.2 | -2.7 | -2.0 | -2.0 | -14.5 | 2.4 |
| HI ($\alpha = 0.5$) | -5.4 | -2.2 | 1.1 | -0.2 | 1.9 | 0.5 | 2.6 |
| HI ($\alpha = 0$) | -8.7 | -1.6 | -0.8 | -0.0 | 3.8 | 3.8 | 3.8 |
| (compensated α) | (0.0) | (0.03) | (0.37) | (0.43) | (0.33) | (0.0) | (0.0) |
| Hearing level of HI | 23.5 | 24.3 | 26.8 | 27.9 | 32.9 | 48.3 | 68.5 |

listeners. It is confirmed that the AT is reasonably simulated independently of the α value, which determines the ratio of HL_{act} and HL_{pas} .

III. NEW IMPLEMENTATION OF WHIS

A new version of WHIS (WHIS_{v30}) is developed based on the algorithm of GCFB_{v23} described in the previous section.

A. Objective of the HL simulator

The first question is what is an ideal HL simulator. The previous version of WHIS (hereafter WHIS_{v22}) was specifically based on the concept of “cancellation of compression” (Irino *et al.*, 2013; Irino and Patterson, 2020; Nagae *et al.*, 2014), where the input sound level was increased as a function of the SPL to virtually reduce the compression in the IO function of an NH listener. This concept is similar to the expansion in the simulation of the loudness

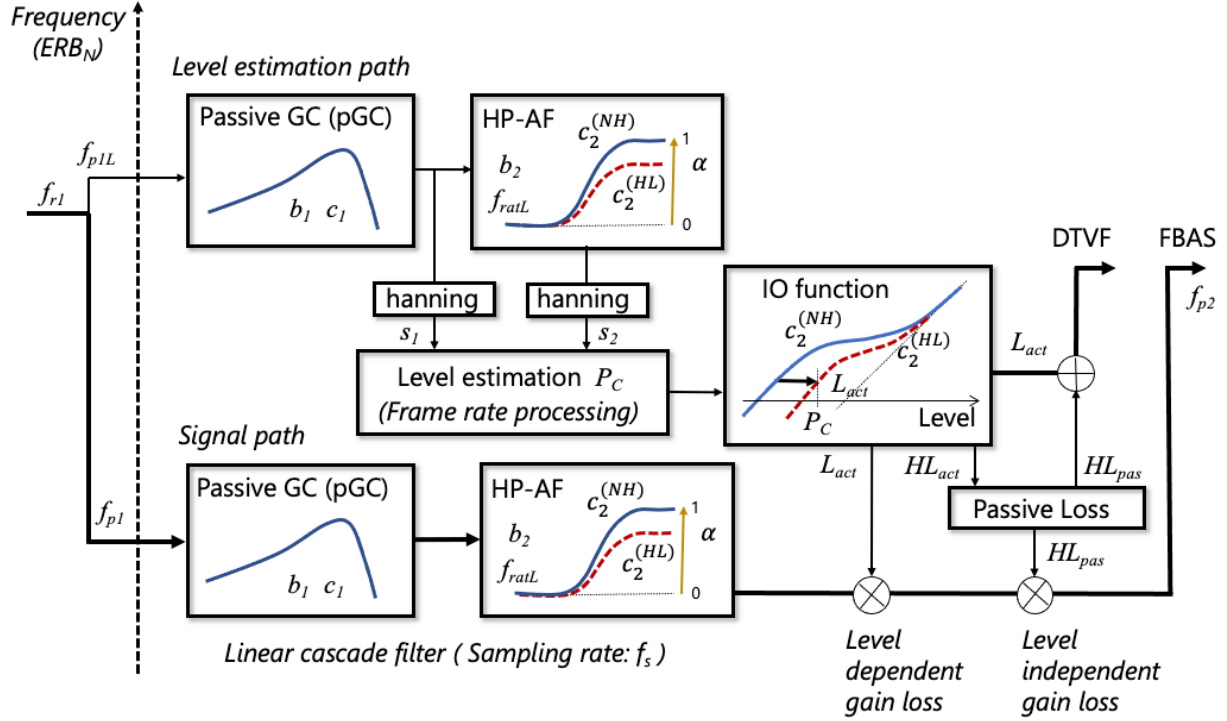


FIG. 5. Block diagram of one channel of analysis section of WHIS_{v30}. Notice that the blocks in the left half is the same as those in GCFB_{v23} (Fig. 1) and the main difference is the use of the IO function instead of the active gain function.

recruitment (Moore and Glasberg, 1993; Villchur, 1974; Zurek and Desloge, 2007). Baer and Moore (1993) added a simulation of the bandwidth widening for HI listeners (Nejime and Moore, 1997).

Although these approaches were practical for simulating specific functions, we started with a more general assumption that an ideal HL simulator can provide an NH listener the same EPs of a specific HI listener by controlling the input sounds. Obviously, a perfect simulation cannot be achieved because of the approximation and limitation of signal processing in GCFB and the lack of knowledge about the dysfunction in the HI listener. However, we assumed that the approximation is possible if certain small errors are allowed. Then, the main issue is the degree of similarity between the EPs of the HI listener and simulated EPs, as described in the next section. The schematic IO function shown in Fig. 4 is found to be useful when considering this approach.

B. Analysis part

Figure 5 shows a block diagram for one channel of the analysis section of WHIS_{v30}. The blocks of the linear cascade filters (pGC + HP-AF) and the level-estimation circuit in the left half are exactly the same as those in GCFB_{v23} as shown in Fig. 1. In practice, the same software is used in this part. The main difference lies in the use of the IO function, as shown in Fig. 4, instead of the active gain function. The IO function is used to estimate the input level from the EP inversely. The EPs of the NH and HI listeners can be calculated by GCFB_{v23} under the NH and HI settings. We assumed that the difference between them corresponds to what WHIS tries to compensate for by converting the input sound.

The IO function, F_{IO} , can be defined as follows:

$$P_{out} = F_{IO}(P_{in}) = G_{act}(P_{in}) + P_{in}, \quad (19)$$

where P_{in} and P_{out} are the input and output levels on a dB scale. G_{act} is the active gain, on a dB scale, which is shown in Fig. 2 and defined in Eq. 16. The conversion from the EP (i.e., the output level) to the input sound level is performed by using the inverse IO function, defined as

$$P_{in} = F_{IO}^{-1}(P_{out}). \quad (20)$$

The algorithms for calculating the signal levels for the simulated HL are formulated as the followings. The passive HL is initially ignored for simplicity, as shown in Fig. 2. The input level necessary to achieve a certain target output level $P_{out}^{(target)}$ (e.g., 10 dB in Fig. 2) for an HI listener can be formulated as:

$$P_{out}^{(target)} = F_{IO}^{(HL)}(P_{in}^{(HL)}), \quad (21)$$

where $F_{IO}^{(HL)}$ is the IO function shown by the red dashed line in Fig. 2, and $P_{in}^{(HL)}$ is the input level for the HI listener. The same output level $P_{out}^{(target)}$ is achieved by an NH listener as

$$P_{out}^{(target)} = F_{IO}^{(NH)}(P_{in}^{(NH)}), \quad (22)$$

where $F_{IO}^{(NH)}$ is the IO function shown by the blue solid line in Fig. 2, and $P_{in}^{(NH)}$ is the input level for the NH listener. As described previously, the objective of WHIS is to equalize the EPs of the HI and NH listeners. The difference between $P_{in}^{(NH)}$ and $P_{in}^{(HL)}$ can be interpreted as active loss, L_{act} , in Fig. 2 in the cochlear input as

$$L_{act} = P_{in}^{(HL)} - P_{in}^{(NH)}. \quad (23)$$

This equation can be rewritten using in Eqs. 20 – 22 as

$$L_{act} = F_{IO}^{(HL)^{-1}}(P_{out}^{(target)}) - F_{IO}^{(NH)^{-1}}(P_{out}^{(target)}). \quad (24)$$

Therefore, the active loss, L_{act} , is calculated at the same output level, $P_{out}^{(target)}$, and represented as a horizontal shift, as shown in Fig. 2.

The WHIS circuit shown in Fig. 5, $P_{out}^{(target)}$ is initially calculated by Eq. 21 using the frame-based level, $P_c(\tau)$, estimated by the level estimation circuit as

$$P_{out}^{(target)} = F_{IO}^{(HL)}(P_c(\tau)). \quad (25)$$

When substituting this equation into Eq. 24, the frame-based active loss, $L_{act}(P_c(\tau))$, can be derived as

$$\begin{aligned} L_{act}(P_c(\tau)) &= F_{IO}^{(HL)^{-1}}\{F_{IO}^{(HL)}(P_c(\tau))\} - F_{IO}^{(NH)^{-1}}\{F_{IO}^{(HL)}(P_c(\tau))\} \\ &= P_c(\tau) - F_{IO}^{(NH)^{-1}}F_{IO}^{(HL)}(P_c(\tau)). \end{aligned} \quad (26)$$

Consequently, the active loss, $L_{act}(P_c(\tau))$, can be simply determined using the composite function, which comprises the IO function of HL, $F_{IO}^{(HL)}$, and the inverse IO function of NH, $F_{IO}^{(NH)^{-1}}$. L_{act} becomes the same as HL_{act} in Eq. 8 when the output level, P_{out} , is zero (i.e., at the AT level), as shown in Fig. 2. Therefore, HL_{act} can be calculated directly from Eq. 24 when $P_c(\tau)$ is set to the AT of the HL listener. Once HL_{act} is determined, the passive loss, HL_{pas} , can be easily determined by using Eq. 8 as

$$HL_{act} = L_{act} \big|_{P_{out}=0} \quad (27)$$

$$HL_{pas} = HL_{total} - HL_{act} \quad (28)$$

The total loss for the HL simulation is derived from these equations as follows:

$$L_{total}(P_c(\tau)) = L_{act}(P_c(\tau)) + HL_{pas}. \quad (29)$$

Note that the signal processing is performed in each filterbank channel n_{ch} with the estimated signal level $P_c(n_{ch}, \tau)$. Equation 29 can be rewritten as follows:

$$L_{total}(n_{ch}, P_c(n_{ch}, \tau)) = L_{act}(n_{ch}, P_c(n_{ch}, \tau)) + HL_{pas}(n_{ch}). \quad (30)$$

Using this equation, the input sound level necessary to simulate the HL can be determined. This algorithm is simpler and more intuitive than that in the previous WHIS (Irimo *et al.*, 2013; Irimo and Patterson, 2020; Nagae *et al.*, 2014). The IO function is operated horizontally as shown in Fig. 2. Although this equation is similar to Eq. 18, the IO function is

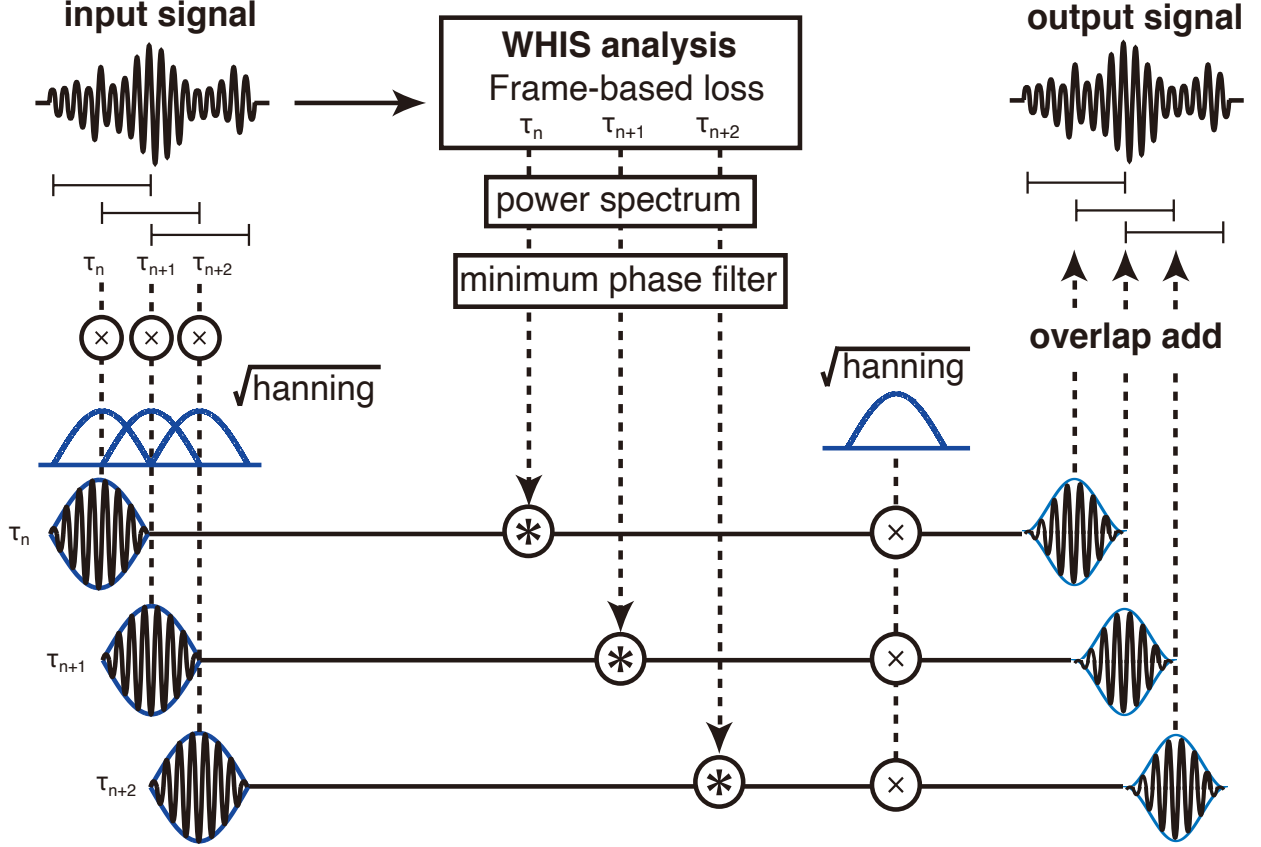


FIG. 6. Signal synthesis using a DTVF.

operated vertically in GCFB. This difference poses the fundamental limit of HL simulators, as described later.

The analysis part in Fig. 5 produces two types of outputs, which correspond to the synthesis methods described in the next section. One of them is the frame-based loss, $L_{total}(n_{ch}, P_c(\tau))$, described in Eq. 30, itself. The other one is the cascade filter output, where the amplitude is dynamically reduced by the resampled version of the total loss $L_{total}(n_{ch}, P_c(n_{ch}, \tau))$.

C. Synthesis part

The simulated HL sounds are synthesized from the analysis part by using two methods.

1. *Direct time-varying filter*

One of the synthesis methods is to apply a nonlinear, time-varying filter to input signals, as used in the previous WHIS (Irino and Patterson, 2020). This is referred to as direct time-varying filtering (DTVf) hereafter. The filter coefficients are calculated from the frame-based loss $L_{total}(n_{ch}, P_c(\tau))$ in Eq. 30. Figure 6 presents a schematic of signal processing. The input signal is divided into frames with a square-root hanning window, $w(t) = \sqrt{0.5 + 0.5 \cos(2\pi t/T)}$ $\{t | -T/2 \leq t \leq T/2\}$, where the frame length, T , is 20 ms and the frame shift is 10 ms. The framed signal is convoluted with a minimum phase filter, which is described in the next paragraph. The filtered signal is windowed again with the same square-root hanning window, $w(t)$. Then, the frames are then overlap-and-added to produce the output signal. When the minimum phase filter is an impulse, the input and output signals are identical, since this procedure is equivalent to processing with a hanning window with half overlapping.

The minimum phase filter is derived from the output of the path labeled “DTVf” in Fig. 5. The frame-based loss $L_{total}(n_{ch}, P_c(\tau))$ in Eq. 30 is interpreted as the spectral distribution of the loss function along the filter channel, n_{ch} (i.e., on the ERB_N number axis). This distribution is converted into the power spectrum on the linear frequency axis by using a warping function from ERB_N number to Hz. Then, the minimum phase filter is derived from this power spectrum using the cepstral method.

WHIS with this DTVf synthesis method is referred to as $WHIS_{v30}^{DTVf}$. The results of the preliminary listening tests indicate that $WHIS_{v30}^{DTVf}$ does not produce noticeable distortion in the output sounds, which is attributable to a single time-varying filter between the input and output for each frame. The filter has a minimum phase response that does not produce pre-echo, which might be perceived as distortion.

However, there is also a disadvantage. It is difficult to introduce the process of temporal smearing because the analysis output is the frame-based loss $L_{total}(n_{ch}, P_c(\tau))$ rather than the EP, which contains the temporal envelope. Although an additional analysis-synthesis filterbank would be applicable to the output sound as post-processing, it becomes inconsistent with the aimed unified framework and results in increasing the distortion.

2. *Filterbank synthesis*

The filterbank synthesis is an alternative method to avoid the disadvantage of DTVf. The output sound is synthesized by an overlap-and-add method, which is commonly used and is similar to that in Irino and Patterson (2006); Irino and Unoki (1999). In the current

implementation for fast processing, the phase delay of the output waveform from the individual filterbank channel is compensated for a constant reciprocal to the center frequency of the corresponding gammachirp filter. Then, the compensated waveforms are added together to synthesize the output. The WHIS obtained with this filterbank analysis-synthesis (FBAS) method is referred to as $\text{WHIS}_{v30}^{\text{FBAS}}$. The process in the single channel is shown in the path labeled “FBAS” in Fig. 5. The amplitude of the output waveform of the linear cascade filter is reduced by $L_{act}(n_{ch}, Pc(\tau))$ and $HL_{pas}(n_{ch})$, as defined in Eq. 30. The process is performed with adequate resampling from the frame rate to the signal sampling rate.

$\text{WHIS}_{v30}^{\text{FBAS}}$ can accommodate the temporal smearing method within a single framework. It is similar to the method used by Drullman *et al.* (1994). The envelope is extracted from the filterbank output by Hilbert transformation or rectification and is filtered using a lowpass filter designed to reduce the temporal resolution. The original carrier component and the reduced envelope are used to synthesize the output sound.

In the preliminary listening tests, the output sounds in $\text{WHIS}_{v30}^{\text{FBAS}}$ are slightly distorted, even without any temporal smearing. The distortion level is slightly higher than that in $\text{WHIS}_{v30}^{\text{DTVF}}$. The phase compensation across the filter channels is not perfectly performed, probably because the temporal response of the cascade filter (pGC + HP-AF) in Fig. 5 is determined not only by the center frequency but also by the compression health α . Thus, to achieve better quality, more sophisticated processing is required.

IV. EVALUATION OF WHIS

We evaluate the simulated HL sounds of speech to clarify the potential and limit of the following four HL simulators: $\text{WHIS}_{v30}^{\text{DTVF}}$, $\text{WHIS}_{v30}^{\text{FBAS}}$, WHIS_{v22} (i.e. the previous version of WHIS), and CamHLS. The HL sounds simulated for an average 80-years-old hearing level (Tsuiki *et al.*, 2002) are analyzed using GCFB_{v23} under the NH setting. For convenience, this process is referred to as “WH-GC(NH)” hereafter. We also analyze the original sounds by using GCFB_{v23} with the same 80-years-old setting. This process is referred to as “GC(HL).” The output representations of WH-GC(NH) and GC(HL) are compared to evaluate the goodness of the simulation. The difference between WH-GC(NH) and GC(HL) is assumed to be greater in the 80-years-old hearing level than in a milder hearing level.

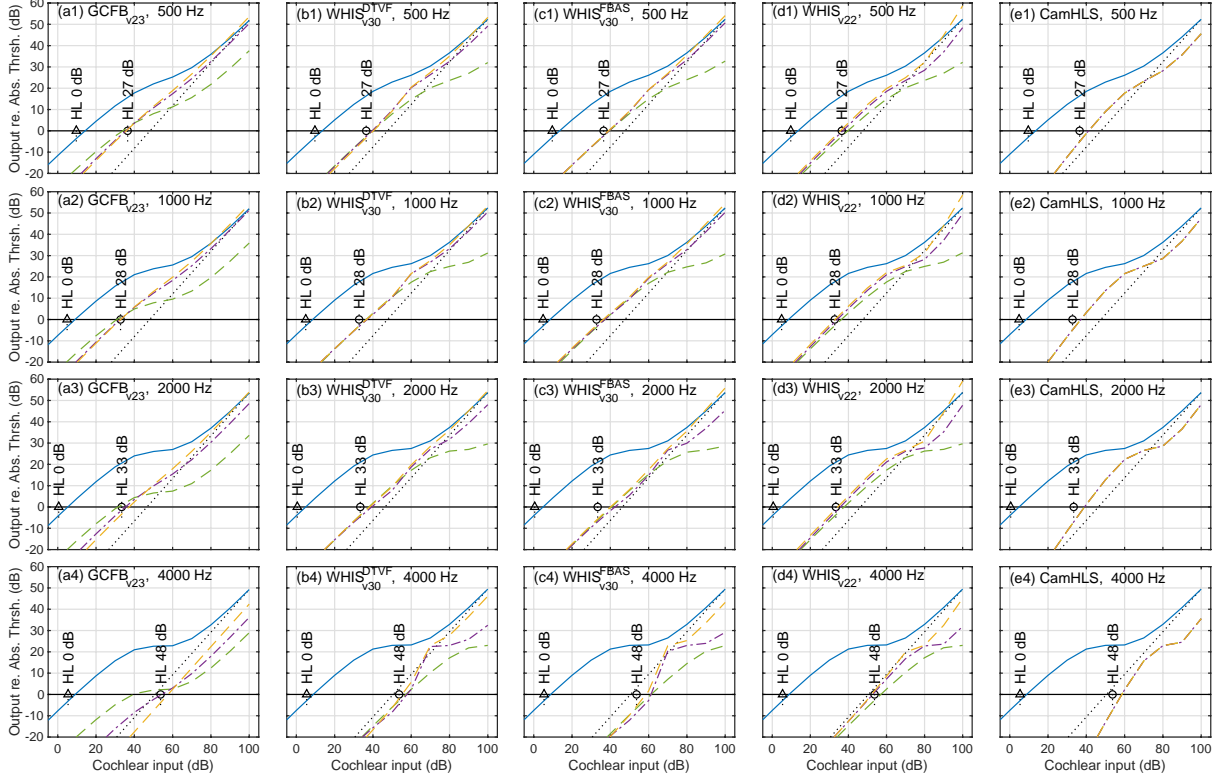


FIG. 7. Simulation results on the IO functions at frequencies of 500, 1000, 2000, and 4000 Hz.

The axes of the figures, the plotted lines, and the HL values are the same as those in Fig. 4.

The panels of (a1)-(a4) show the IO functions of GC(HL), which are the same as those shown

in Fig. 4 for corresponding frequencies. The other panels show the IO functions of WH-GC(NH)

with $\text{WHIS}_{v30}^{\text{D}_{\text{TVF}}}$ ((b1)-(b4)) , with $\text{WHIS}_{v30}^{\text{F}_{\text{ABS}}}$ ((c1)-(c4)) , with WHIS_{v22} ((d1)-(d4)), and with

CamHLS ((e1)-(e4)). Blue solid line: Average NH. Green dashed line: HL with the compression

health α of 1. Purple dashed-and-dotted line: HL with α of 0.5. Orange dashed line: HL with α

of 0. Black dotted line: The linear relationship (1:1).

A. IO function

The IO functions are calculated by using short sinusoids, which were used for producing Fig. 4. Figure 7 shows the simulation results. The panels of (a1)-(a4) show the IO functions of GC(HL) at the frequencies of 500, 1000, 2000, and 4000 Hz. These panels are identical to those shown in Fig. 4 for the corresponding frequencies. The IO functions in panels (b1)-(b4) are for WH-GC(NH) with $\text{WHIS}_{v30}^{\text{DTVf}}$; those in (c1)-(c4) are for WH-GC(NH) with $\text{WHIS}_{v30}^{\text{FABS}}$; those in (d1)-(d4) are for WH-GC(NH) with WHIS_{v22} ; and those in (e1)-(e4) are for WH-GC(NH) with CamHLS.

1. Comparison with GCFB

First, let us compare panels (a1)-(a4) for GC(HL) and (b1)-(b4) for WH-GC(NH) with $\text{WHIS}_{v30}^{\text{DTVf}}$. The IO functions of the NH conditions (blue solid lines) are clearly the same at the same frequency because no HL processing is performed in WH-GC(NH). The IO functions for α of 0.0 and 0.5 (orange and purple lines, respectively) are similar except for 4000 Hz. The major differences are observed at $\alpha = 1.0$ (green dashed lines). The locations of the compressive regions are higher in WH-GC(NH) than in GC(HL), which can be explained by the difference in the gain control. The output levels in panels (a1)-(a4) are calculated from $G_{\text{total}}(n_{ch}, P_c(\tau))$ in Eq. 18, which operates the IO functions vertically, as shown in Fig. 2. At $\alpha = 1.0$, the NH IO functions (blue line) are shifted downward for $L_{pas}(n_{ch})$ to the HL IO functions (green dashed line). In contrast, the operations in any HL simulators are completely different because they solely control the input signal levels and cannot touch the output levels directly. The input levels in $\text{WHIS}_{v30}^{\text{DTVf}}$ are controlled by $L_{\text{total}}(n_{ch}, P_c(\tau))$ in Eq. 30, which operates the IO functions horizontally, as shown in Fig. 2. At $\alpha = 1.0$, the NH IO functions (blue solid line) are shifted rightward for $HL_{pas}(n_{ch})$ to the HL IO functions (green dashed line). As a result, the IO functions are different in panels (a1)-(a4) and (b1)-(b4). The degree of inconsistency is smaller at $\alpha \leq 0.5$. This is because, at this value, the IO functions are less compressive, and the vertical shift induced by the passive loss $L_{pas}(n_{ch})$ in Eq. 18 and the horizontal shift induced by the passive loss $HL_{pas}(n_{ch})$ in Eq. 30 are relatively smaller as compared to the case of $\alpha = 1$. The results reveal the fundamental limit of any existing HL simulator.

2. Comparison between the HL simulators

The IO functions in panels (c1)-(c4) for WH-GC(NH) with $\text{WHIS}_{v30}^{\text{FBAS}}$ in Fig. 7 are the same as those in panels (b1)-(b4) for WH-GC(NH) with $\text{WHIS}_{v30}^{\text{DTVf}}$. This means that the synthesis parts in $\text{WHIS}_{v30}^{\text{DTVf}}$ and $\text{WHIS}_{v30}^{\text{FBAS}}$ do not affect the results when the sinusoids are processed.

The differences between panels (d1)-(d4) for WH-GC(NH) with WHIS_{v22} and panels (b1)-(b4) for WH-GC(NH) with $\text{WHIS}_{v30}^{\text{DTVf}}$ are mainly observed at $\alpha = 0.5$, where the input levels exceed 80 dB. However, the IO functions at $\alpha = 1.0$ and $\alpha = 0.0$ are very similar. The difference at $\alpha = 0.5$ is attributable to that in the definitions of α in WHIS_{v30} (Eq. 9) and in WHIS_{v22} (Irino and Patterson, 2020), although the range is the same $\{\alpha | 0.0 \leq \alpha \leq 1.0\}$. Therefore, the output of WHIS_{v22} might be similar to that of WHIS_{v30} when the α value is adequately converted. The results imply that the perceptual experiments performed using WHIS_{v22} can be interpreted consistently with those performed using WHIS_{v30} .

There is a single IO function in WH-GC(NH) with CamHLS for each frequency, as shown in panels (e1)-(e4). Under the default setting, the IO function is automatically determined from the given audiogram. The IO functions are similar to those in WHIS_{v30} at $\alpha = 0.5$. This means that both WHIS_{v30} and CamHLS can simulate the loudness recruitment.

B. Distance between auditory spectrograms

We evaluate the HL simulators using speech sounds because such nonlinear systems cannot be evaluated sufficiently by simple sinusoids. The auditory spectrograms calculated from GCFB_{v23} are used for the evaluation.

1. Method

The speech sounds are analyzed using the GC(HL) process, as described above, to derive the reference auditory spectrogram $S(n_{ch}, \tau)_{GC(HL)}$, where n_{ch} is the filterbank channel and τ is the frame time. The frame window length is 1.0 ms, and the frame shift is 0.5 ms. The input speech sounds are normalized at the SPLs of 50 and 80 dB in L_{eq} (i.e., rms level). The α values are set to 1.0, 0.5, and 0.0. For the analysis, 20 speech sounds pronounced by two male and two female speakers are drawn from the Japanese word database FW07 (Amano *et al.*, 2007).

The auditory spectrograms of the simulated HL sounds $S(n_{ch}, \tau)_{GC(NH)}^{WH}$ are calculated by the WH-GC(NH) process. The spectral distance between $S(n_{ch}, \tau)_{GC(NH)}^{WH}$ and $S(n_{ch}, \tau)_{GC(HL)}$ is used for a goodness measure of the HL simulation. The simulation result is good enough if the distance is very small. We defined the normalized spectral distance d_{sp} (dB) as

$$d_{sp} = 10 \log_{10} \left[\frac{\sum_{n_{ch}} \sum_{\tau} \{S(n_{ch}, \tau + \Delta\tau)_{GC(NH)}^{WH} - S(n_{ch}, \tau)_{GC(HL)}\}^2}{\sum_{n_{ch}} \sum_{\tau} S(n_{ch}, \tau)_{GC(HL)}^2} \right]. \quad (31)$$

where $\Delta\tau$ is the frame shift which yields the minimum distance. This is necessary because the start time of the HL-simulated sound might be different from that of the original sound. $\Delta\tau$ is searched within a limited range.

Moreover, noisy sounds are analyzed using the GC(HL) process to estimate the degree of distortion. Pink noise is added to the original speech sound with SNRs of +3, 0, and -3 dB. The derived auditory spectrogram is substituted for $S(n_{ch}, \tau)_{GC(NH)}^{WH}$ in Eq. 31. Therefore, in this case, the d_{sp} values are calculated between the noisy and clean speech sounds. The d_{sp} values can help interpret the results, although the nonlinear distortion and the additive noise are completely different in perceptual impression.

2. Results

Figure 8 shows the mean and standard deviation (SD) of the d_{sp} values. We compare WHIS_{v30}^{DTVF}, WHIS_{v30}^{FBAS}, and WHIS_{v22} in the WHIS family and CamHLS. The d_{sp} values of noisy sounds at the SNRs of 3, 0, and -3 dB are also plotted on the right to obtain information about the degree of the distortion.

a. ANOVA. We conduct a three-factor ANOVA on the HL simulation condition, the SPL, and the α value. The results show significant differences in the main effect and in interaction ($p < 10^{-10}$ under any condition). We then analyze the differences in the individual factors.

b. Difference between the SPLs and the α conditions. The spectral distances in the WHIS family at $\alpha = 1$ were approximately 3 dB greater under 80 dB condition (panel (d)) than under 50 dB condition (panel (a)). This is probably because the IO functions at $\alpha = 1$ are largely different between the GC(HL) and WH-GC(NH) conditions at a high SPL, as shown in Fig. 7. There are various differences between the two SPL conditions at $\alpha = 0$ and $\alpha = 0.5$.

c. Difference between the WHIS family and CamHLS. The spectral distances are always greater in CamHLS than in the WHIS family, as observed in the all panels. This is

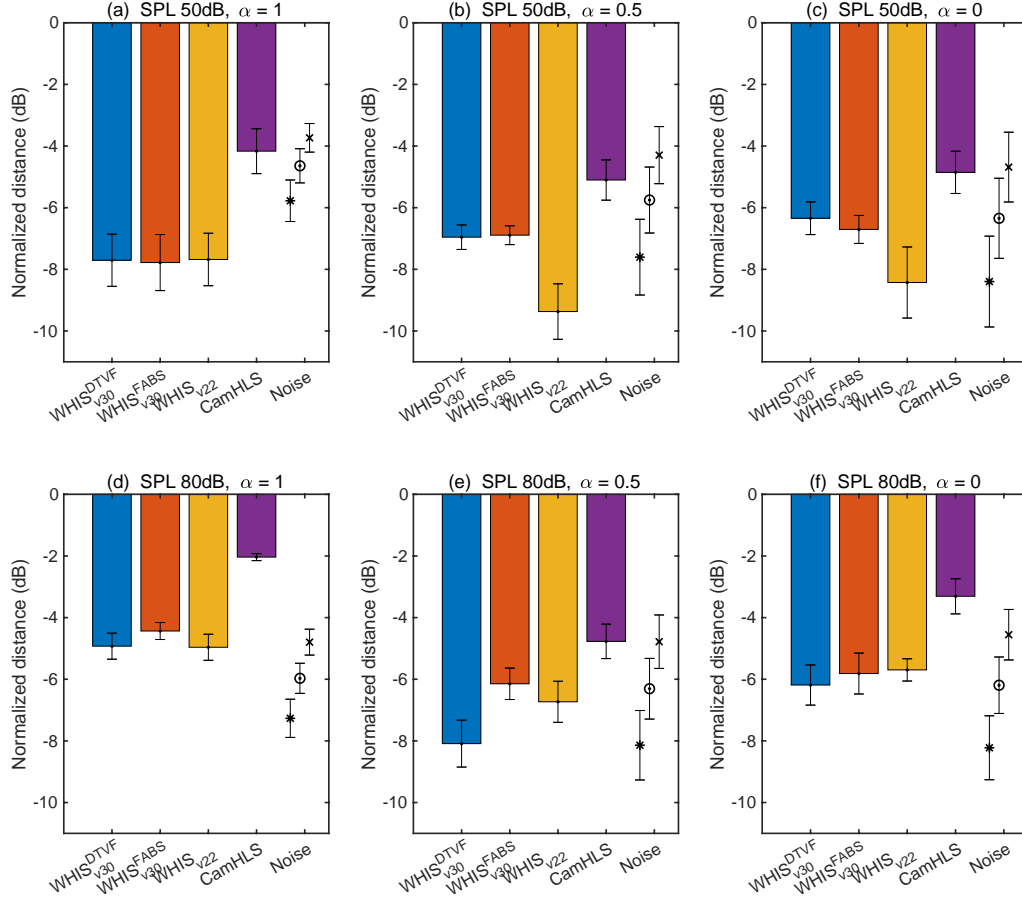


FIG. 8. Spectral distance d_{sp} in Eq. 31. Bars and error bars represent the mean and standard deviation (SD) of d_{sp} . The conditions for the SPL and α are labeled at the top of each panel. The HL simulator conditions are $\text{WHIS}_{v30}^{\text{DTVf}}$ (blue), $\text{WHIS}_{v30}^{\text{FBAS}}$ (red), WHIS_{v22} (orange), and CamHLS (purple). The d_{sp} values for the noisy sounds when the SNRs are 3 dB(*), 0 dB(o), and -3 dB (\times) are also plotted in the rightmost part.

probably because spectral smearing is introduced into CamHLS to simulate the bandwidth widening in the HI listeners (Baer and Moore, 1993, 1994). The process of the spectral smearing produces distortion, which is described as “The ‘spectral smearing’ software has the perceptual effect of adding a certain ‘grittiness’ to the audio quality” in the software (control.impaired.ear.m). This distortion can be avoided and the spectral distance can be reduced by removing the spectral smearing process.

d. Difference within the WHIS family. The distances are smaller in WHIS_{v22} than in $\text{WHIS}_{v30}^{\text{DTVf}}$ and $\text{WHIS}_{v30}^{\text{FBAS}}$ under the 50 dB condition and at $\alpha = 0.5$ and $\alpha = 0$ (panels (b) and (c)). In contrast, the distance is the smallest in $\text{WHIS}_{v30}^{\text{DTVf}}$ under the 80 dB condition and at $\alpha = 0.5$ (panel (e)). In the other conditions, the distances in $\text{WHIS}_{v30}^{\text{DTVf}}$ and $\text{WHIS}_{v30}^{\text{FBAS}}$ are approximately the same.

One of the purposes of the HL simulator is to provide insight into how loud the sounds are required for the HI listeners. $\text{WHIS}_{v30}^{\text{DTVf}}$ might be advantageous for this purpose because the distortion is the minimum under the 80 dB condition. However, the differences among $\text{WHIS}_{v30}^{\text{DTVf}}$, $\text{WHIS}_{v30}^{\text{FBAS}}$, and WHIS_{v22} are small; they seem to be compatible in general.

e. Difference between the HL-simulated sounds and the noisy sounds. It is not easy to interpret whether the value of the spectral distance is sufficiently small. We calculate the spectral distances between the clean and noisy sounds at SNRs of 3, 0, and -3 dB under the GC(HL) condition. The results are shown in the rightmost part in each panel. The spectral distances of the WHIS family are generally smaller than or equal to those of the noisy sounds at 0 dB SNR. In the case of panel (d), the spectral distance is almost the same as that of the noisy sounds at -3 dB SNR. Therefore, the distances are not very small. However, the distortion and noise components in the sounds simulated by WHIS are not perceptually salient, unlike the additive noise sounds. WHIS does not produce any “grittiness” component. WHIS accomplishes the HL simulation up to this quality.

V. DISCUSSION

A. Fundamental limit of the HL simulators

The results of the IO function shown in Fig. 7 and the spectral distance shown in Fig. 8 demonstrate that the HL simulation cannot be accurately performed when α is close to 1, or in other words, when the active process including the OHC function is healthy. This implies that it is difficult to simulate hidden HL (Lieberman, 2015), including synaptopathy (Sergeyenko *et al.*, 2013), when the OHC function is diagnosed as healthy. This is a fundamental limit of any existing HL simulator as well as WHIS. To overcome this problem, it is essential to simulate the compression just above the output level of 0 dB, as shown in Fig. 4 and in Fig. 7 (a1)-(a4). However, this is not easy to achieve and remains problematic.

In contrast, the HLs of many elderly HI listeners might be caused by the dysfunctions in both the active and passive processes. At α less than 1, the HL simulation improves,

as shown in Fig. 7. In any case, it is essential to estimate the ratio between the active and passive HLs, as discussed in the next section.

The results also demonstrate that passive devices, such as earplugs and graphic equalizers, could not simulate the cochlear HL. The passive attenuation simply moves the NH IO function rightward, as shown by the $\alpha = 1$ line in Fig. 7. Nonlinear processing, such as that implemented in WHIS, is essential for cochlear HL simulation.

B. Estimation of the active and passive HLs

It is essential to estimate the α value in Eq. 9 or the ratio of HL_{act} and HL_{pas} in Eq. 8 for reliable HL simulations. The audiogram does not provide any information about this. The estimation of the IO function can resolve this problem. The compression in the IO function is measured psychoacoustically by using the forward masking paradigms, such as the growth-of-masking curve method (Oxenham and Plack, 1997) and the temporal-masking curve method (Nelson *et al.*, 2001). An alternative method is to estimate an auditory filter using simultaneous NN masking experiments (Patterson, 1976) with various stimulus levels. The level dependence of the auditory filter provides a good estimate of the IO function (Baker and Rosen, 2002; Irino and Patterson, 2001; Patterson *et al.*, 2003).

However, these psychoacoustic methods require many measurement points for reliable estimation. They require heavy experiments that take much longer than the normal tests performed in clinical sites. Therefore, it is not very easy to estimate the parameter of a target HI listener, and a method as simple as audiometry is required to estimate the α value or the ratio of HL_{act} and HL_{pas} .

C. Applications of WHIS

There are many potential applications of the HL simulators. For example, Zurek and Desloge (2007) indicated that the HL and prosthesis simulations are useful in counseling, hearing aid fitting, training, hearing conservation, testing warning signals, and setting job requirements.

An important applications includes psychoacoustic experiments using speech and environmental sounds, as indicated in the Introduction. For this purpose, WHIS has been developed to minimize the distortion and noise, which might affect the experimental results. Several experiments performed with WHIS are introduced in this section as examples for further studies. For example, Matsui *et al.* (2016) used an early version of WHIS to measure

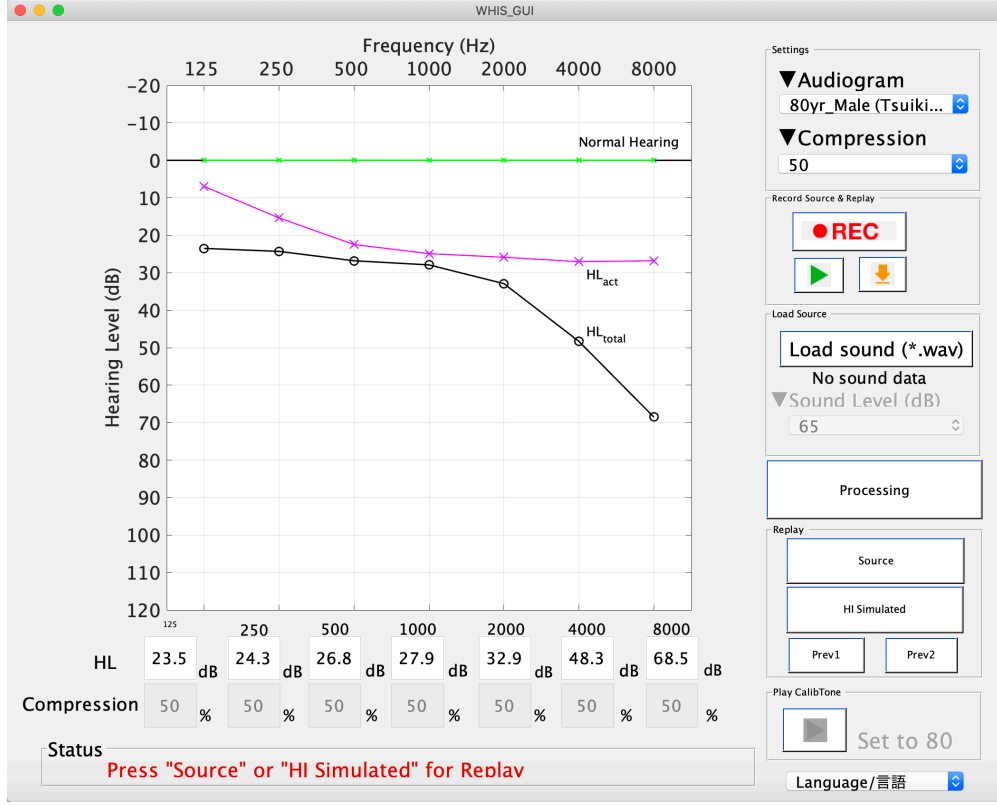


FIG. 9. GUI of WHIS

the effect of compression loss on syllable recognition. [Grimault *et al.* \(2018\)](#) measured the NN thresholds and estimated the auditory filter using a real-time HL simulator based on GCFB. In addition to the perceptual experiments, [Irino *et al.* \(2020\)](#) used WHIS_{v22} in vocal self-training experiments to determine whether the speech clarity towards HI listeners was improved. Recently, [Irino *et al.* \(2022\)](#) performed speech intelligibility experiments in the laboratory and crowdsourced remote environments using WHIS_{v30}^{DTVF} to clarify the effects of the listening conditions.

The stimuli in these experiments are prepared in advance using a batch program in WHIS. A graphical user interface (GUI) shown in Fig. 9 is used to provide NH listeners the experience of the difficulties of HI listeners interactively. WHIS with the GUI has been used in a training program for speech-language-hearing therapists for several years ([Hasegawa *et al.*, 2019](#)). The GUI has a main audiogram panel and several sets of control buttons. After calibration of the SPL, the user chooses an audiogram and a value of the compression health α in percentage. The audiogram is then plotted with the black line labeled with HL_{total} in the main panel. In addition, HL_{act} is plotted with the magenta line. At $\alpha = 1$, the magenta line coincides with the green line (i.e. the hearing level of 0 dB). The difference between the HL_{total} and HL_{act} lines corresponds to HL_{pas} , which is calculated from Eq. 8.

Using several buttons, we can record speech sound or load prerecorded speech, and then listen to the HL-simulated sound.

VI. CONCLUSIONS

In this study, WHIS_{v30} was developed based on GCFB_{v22}, which was updated to incorporate fast frame-based processing, the AT, the audiogram of a target HI listener, and the parameter to control the IO function. In GCFB_{v22}, the compression health α was also introduced as an HP-AF parameter to control the degree of compression in the cochlear IO functions, which range from NH listeners to HI listeners. The total HL in the audiogram HL_{total} was assumed to be the sum of the active HL HL_{act} and the passive HL HL_{pas} on a dB scale. As a result, the various IO functions were derived in accordance with α without much changes in the AT values. The cascade of pGC and HP-AF filters in each GCFB_{v22} channel was approximated using a linear filter to fulfill the fast processing required in WHIS. Thus, the filter shape and bandwidth were controlled by α but not by SPL. The estimation of α for the target HI listener and the introduction of the level dependence remain problems for future studies.

WHIS_{v30} was developed to provide NH listeners approximately the same EPs as those of HI listeners. The output level for the HL simulator could be controlled by a composite function of the IO function of an NH listener and the inverse IO function of a target HI listener. The analysis part of WHIS_{v30} was almost the same as that of GCFB_{v22}, except for using the IO function instead of using the gain function. We proposed two synthesis methods: DTVF for perceptually small distortion and FBAS for additional HI simulations, including temporal smearing.

Finally, we evaluated the WHIS family and CamHLS in terms of differences in the IO function and the spectral distance. The IO functions were well-simulated at $\alpha \leq 0.5$. This was not the case at $\alpha = 1$. Thus, it is difficult to simulate the HL caused by synaptopathy when the OHC is sufficiently healthy. This is a fundamental limit of the existing HL simulator and WHIS. To overcome this problem, it is essential to precisely simulate the compression just above the AT. This also remains a problem for the future studies. The spectral distortion was smaller in the WHIS family than in CamHLS, and WHIS_{v30} was virtually compatible with WHIS_{v23}. The software of WHIS_{v30} and GCFB_{v22} is available in our GitHub repository ([Irino and Yamamoto, 2018](#)).

ACKNOWLEDGEMENTS

This work was supported by JSPS KAKENHI Grant Numbers JP16H01734, JP18K10708, JP21H03468, and JP21K19794. The author wishes to thank Dr. Michael A. Stone for providing the CamHLS software and Dr. Yasuki Murakami for valuable comments on the earlier draft.

- Amano, S., Kondo, T., Sakamoto, S., and Suzuki, Y. (2007). “Ntt - tohoku university familiarity-controlled word lists 2007 (fw07)” <https://doi.org/10.32130/src.FW07>.
- ANSI/ASA S3. 6 - 2018 (2018). “Specification for audiometers” <https://webstore.ansi.org/standards/asa/ansiasas32018>.
- Bacon, S. P., and Viemeister, N. F. (1985). “Temporal modulation transfer functions in normal-hearing and hearing-impaired listeners,” *Audiology* **24**(2), 117–134, doi: [10.3109/00206098509081545](https://doi.org/10.3109/00206098509081545).
- Baer, T., and Moore, B. C. (1993). “Effects of spectral smearing on the intelligibility of sentences in noise,” *The Journal of the Acoustical Society of America* **94**(3), 1229–1241, doi: [10.1121/1.408176](https://doi.org/10.1121/1.408176).
- Baer, T., and Moore, B. C. (1994). “Effects of spectral smearing on the intelligibility of sentences in the presence of interfering speech,” *The Journal of the Acoustical Society of America* **95**(4), 2277–2280, doi: [10.1121/1.408640](https://doi.org/10.1121/1.408640).
- Baker, R. J., and Rosen, S. (2002). “Auditory filter nonlinearity in mild/moderate hearing impairment,” *The Journal of the Acoustical Society of America* **111**(3), 1330–1339, doi: [10.1121/1.1448516](https://doi.org/10.1121/1.1448516).
- Clarity Challenge, C. (2021). “Clarity challenge” <https://claritychallenge.org>, (Last: 21 Apr 2022).
- Drullman, R., Festen, J. M., and Plomp, R. (1994). “Effect of temporal envelope smearing on speech reception,” *The Journal of the Acoustical Society of America* **95**(2), 1053–1064, doi: [10.1121/1.408467](https://doi.org/10.1121/1.408467).
- Glasberg, B. R., and Moore, B. C. (1986). “Auditory filter shapes in subjects with unilateral and bilateral cochlear impairments,” *The Journal of the Acoustical Society of America* **79**(4), 1020–1033.
- Glasberg, B. R., and Moore, B. C. (2006). “Prediction of absolute thresholds and equal-loudness contours using a modified loudness model,” *The Journal of the Acoustical Society of America* **120**(2), 585–588, doi: [10.1121/1.2214151](https://doi.org/10.1121/1.2214151).

- Grimault, N., Irino, T., Dimachki, S., Corneyllie, A., Patterson, R. D., and Garcia, S. (2018). “A real time hearing loss simulator,” *Acta Acustica united with Acustica* **104**(5), 904–908, doi: [10.3813/AAA.919252](https://doi.org/10.3813/AAA.919252).
- Hasegawa, J., Hashi, M., Matsui, T., and Irino, T. (2019). “Application of a hearing loss simulator to education, clinic, and research and its evaluation by speech-language-hearing therapists (in japanese),” in *Proc. Japanese Association of Speech-Language-Hearing Therapists*, pp. 1–P03–4.
- Hu, H., Sang, J., Lutman, M. E., and Bleeck, S. (2011). “Simulation of hearing loss using compressive gammachirp auditory filters,” in *2011 IEEE International Conference on Acoustics, Speech and Signal Processing (ICASSP)*, IEEE, pp. 5428–5431.
- Irino, T., Fukawatase, T., Sakaguchi, M., Nisimura, R., Kawahara, H., and Patterson, R. D. (2013). “Accurate estimation of compression in simultaneous masking enables the simulation of hearing impairment for normal-hearing listeners,” in *Basic Aspects of Hearing* (Springer), pp. 73–80, doi: [10.1007/978-1-4614-1590-9_9](https://doi.org/10.1007/978-1-4614-1590-9_9).
- Irino, T., Higashiyama, S., and Yoshigi, H. (2020). “Speech clarity improvement by vocal self-training using a hearing impairment simulator and its correlation with an auditory modulation index,” in *Proc. Interspeech 2020*, pp. 2507–2511, doi: [10.21437/Interspeech.2020-1081](https://doi.org/10.21437/Interspeech.2020-1081).
- Irino, T., and Patterson, R. D. (1997). “A time fomain, level-dependent auditory filter: the gammachirp,” *The Journal of the Acoustical Society of America* **101**(1), 412–419, doi: [10.1121/1.417975](https://doi.org/10.1121/1.417975).
- Irino, T., and Patterson, R. D. (2001). “A compressive gammachirp auditory filter for both physiological and psychophysical data,” *The Journal of the Acoustical Society of America* **109**(5), 2008–2022.
- Irino, T., and Patterson, R. D. (2006). “A dynamic compressive gammachirp auditory filterbank,” *IEEE transactions on audio, speech, and language processing* **14**(6), 2222–2232, doi: [10.1109/TASL.2006.874669](https://doi.org/10.1109/TASL.2006.874669).
- Irino, T., and Patterson, R. D. (2020). “The gammachirp auditory filter and its application to speech perception,” *Acoust. Sci. and Technol.* **41**(1), 99–107, doi: [10.1250/ast.41.99](https://doi.org/10.1250/ast.41.99).
- Irino, T., Tamaru, H., and Yamamoto, A. (2022). “A new implementation of hearing impairment simulator whis and the effect of peripheral dysfunction on speech intelligibility (in japanese),” in *Proc. Acoustical Society of Japan, Spring Meeting*, pp. 665–668.
- Irino, T., and Unoki, M. (1999). “An analysis/synthesis auditory filterbank based on an iir implementation of the gammachirp,” *Journal of the Acoustical Society of Japan (E)* **20**(6), 397–406, doi: [/10.1250/ast.20.397](https://doi.org/10.1250/ast.20.397).

- Irino, T., and Yamamoto, K. (2018). “Amlab-wakayama github repository” <https://github.com/AMLAB-Wakayama/>, (Last: 21 Apr 2022).
- Lieberman, M. C. (2015). “Hidden hearing loss,” *Scientific American* **313**(2), 48–53, <https://www.jstor.org/stable/26046106>.
- Matsui, T., Irino, T., Nagae, M., Kawahara, H., and Patterson, R. D. (2016). “The effect of peripheral compression on syllable perception measured with a hearing impairment simulator,” in *Physiology, Psychoacoustics and Cognition in Normal and Impaired Hearing* (Springer, Cham), pp. 307–314, doi: [10.1007/978-3-319-25474-6](https://doi.org/10.1007/978-3-319-25474-6).
- Moore, B. C., and Glasberg, B. R. (1993). “Simulation of the effects of loudness recruitment and threshold elevation on the intelligibility of speech in quiet and in a background of speech,” *The Journal of the Acoustical Society of America* **94**(4), 2050–2062, doi: [10.1121/1.407478](https://doi.org/10.1121/1.407478).
- Moore, B. C., Glasberg, B. R., and Baer, T. (1997). “A model for the prediction of thresholds, loudness, and partial loudness,” *Journal of the Audio Engineering Society* **45**(4), 224–240, <http://www.aes.org/e-lib/browse.cfm?elib=10272>.
- Moore, B. C. J. (2013). *An introduction to the psychology of hearing*, 6th ed. (Brill, Leiden, The Netherlands), <https://brill.com/view/title/24210>.
- Nagae, M., Irino, T., Nisimura, R., Kawahara, H., and Patterson, R. D. (2014). “Hearing impairment simulator based on compressive gammachirp filter,” in *Signal and Information Processing Association Annual Summit and Conference (APSIPA), 2014 Asia-Pacific*, IEEE, pp. 1–4, doi: [10.1109/APSIPA.2014.7041579](https://doi.org/10.1109/APSIPA.2014.7041579).
- Nejime, Y., and Moore, B. C. (1997). “Simulation of the effect of threshold elevation and loudness recruitment combined with reduced frequency selectivity on the intelligibility of speech in noise,” *The Journal of the Acoustical Society of America* **102**(1), 603–615, doi: [10.1121/1.419733](https://doi.org/10.1121/1.419733).
- Nelson, D. A., Schroder, A. C., and Wojtczak, M. (2001). “A new procedure for measuring peripheral compression in normal-hearing and hearing-impaired listeners,” *The Journal of the Acoustical Society of America* **110**(4), 2045–2064, doi: [10.1121/1.1404439](https://doi.org/10.1121/1.1404439).
- Oxenham, A. J., and Plack, C. J. (1997). “A behavioral measure of basilar-membrane nonlinearity in listeners with normal and impaired hearing,” *The Journal of the Acoustical Society of America* **101**(6), 3666–3675, doi: [10.1121/1.418327](https://doi.org/10.1121/1.418327).
- Patterson, R. D. (1976). “Auditory filter shapes derived with noise stimuli,” *The Journal of the Acoustical Society of America* **59**(3), 640–654, doi: [10.1121/1.380914](https://doi.org/10.1121/1.380914).
- Patterson, R. D., Nimmo-Smith, I., Weber, D. L., and Milroy, R. (1982). “The deterioration of hearing with age: Frequency selectivity, the critical ratio, the audiogram, and speech threshold,” *The Journal of the Acoustical Society of America* **72**(6), 1788–1803, doi: [10.1121/1.389114](https://doi.org/10.1121/1.389114).

[1121/1.388652](#).

- Patterson, R. D., Unoki, M., and Irino, T. (2003). “Extending the domain of center frequencies for the compressive gammachirp auditory filter,” *The Journal of the Acoustical Society of America* **114**(3), 1529–1542, doi: [10.1121/1.1600720](#).
- Sergeyenko, Y., Lall, K., Liberman, M. C., and Kujawa, S. G. (2013). “Age-related cochlear synaptopathy: an early-onset contributor to auditory functional decline,” *Journal of Neuroscience* **33**(34), 13686–13694.
- Stone, M. A., and Moore, B. C. (1999). “Tolerable hearing aid delays. i. estimation of limits imposed by the auditory path alone using simulated hearing losses,” *Ear and Hearing* **20**(3), 182–192, https://journals.lww.com/ear-hearing/Abstract/1999/06000/Tolerable_Hearing_Aid_Delays__I__Estimation_of.2.aspx.
- Tsuiki, T., Sasamori, S., Minami, Y., Ichinohe, T., Murai, K., Murai, S., and Kawashima, H. (2002). “Age effect on hearing: a study on japanese,” *Audiology Japan* (in Japanese) **45**(3), 241–250, doi: [10.4295/audiology.45.241](#).
- Unoki, M., Irino, T., Glasberg, B., Moore, B. C., and Patterson, R. D. (2006). “Comparison of the roex and gammachirp filters as representations of the auditory filter,” *The Journal of the Acoustical Society of America* **120**(3), 1474–1492.
- Villchur, E. (1974). “Simulation of the effect of recruitment on loudness relationships in speech,” *The Journal of the Acoustical Society of America* **56**(5), 1601–1611, doi: [10.1121/1.1903484](#).
- Zurek, P. M., and Desloge, J. G. (2007). “Hearing loss and prosthesis simulation in audiology,” *The Hearing Journal* **60**(7), 32–38, doi: [10.1097/01.HJ.0000281789.77088.b6](#).